

# UCLA

## UCLA Previously Published Works

### Title

Deep in the brain: Changes in subcortical function immediately preceding a migraine attack

### Permalink

<https://escholarship.org/uc/item/14c2q41d>

### Journal

Human Brain Mapping, 39(6)

### ISSN

1065-9471

### Authors

Meylakh, Noemi  
Marciszewski, Kasia K  
Di Pietro, Flavia  
[et al.](#)

### Publication Date

2018-06-01



### DOI

10.1002/hbm.24030

Peer reviewed

## RESEARCH ARTICLE

# Deep in the brain: Changes in subcortical function immediately preceding a migraine attack

Noemi Meylakh<sup>1</sup> | Kasia K. Marciszewski<sup>1</sup> | Flavia Di Pietro<sup>1</sup> |  
Vaughan G. Macefield<sup>2</sup> | Paul M. Macey<sup>3</sup>  | Luke A. Henderson<sup>1</sup> 

<sup>1</sup>Department of Anatomy and Histology, University of Sydney, Sydney, New South Wales 2006, Australia

<sup>2</sup>School of Medicine, Western Sydney University, Sydney, New South Wales, Australia

<sup>3</sup>UCLA School of Nursing and Brain Research Institute, University of California, Los Angeles, California 90095

## Correspondence

Luke A. Henderson, Department of Anatomy and Histology, F13, University of Sydney, Sydney, New South Wales 2006, Australia.

Email: lukeh@anatomy.usyd.edu.au

## Funding information

National Health and Medical Research Council of Australia, Grant/Award Numbers: 1032072, 1059182

## Abstract

The neural mechanism responsible for migraine remains unclear. While the role of an external trigger in migraine initiation remains vigorously debated, it is generally assumed that migraineurs display altered brain function between attacks. This idea stems from relatively few brain imaging studies with even fewer studies exploring changes in the 24 h period immediately prior to a migraine attack. Using functional magnetic resonance imaging, we measured infra-slow oscillatory activity, regional homogeneity, and connectivity strengths of resting activity in migraineurs directly before ( $n = 8$ ), after ( $n = 11$ ), and between migraine attacks ( $n = 26$ ) and in healthy control subjects ( $n = 78$ ). Comparisons between controls and each migraine group and between migraine groups were made for each of these measures. Directly prior to a migraine, increased infra-slow oscillatory activity occurred in brainstem and hypothalamic regions that also display altered activity during a migraine itself, that is, the spinal trigeminal nucleus, dorsal pons, and hypothalamus. Furthermore, these midbrain and hypothalamic sites displayed increased connectivity strengths and regional homogeneity directly prior to a migraine. Remarkably, these resting oscillatory and connectivity changes did not occur directly after or between migraine attacks and were significantly different to control subjects. These data provide evidence of altered brainstem and hypothalamic function in the period immediately before a migraine and raise the prospect that such changes contribute to the expression of a migraine attack.

## KEYWORDS

hypothalamus, infra-slow oscillations, periaqueductal gray matter, spinal trigeminal nucleus

## 1 | INTRODUCTION

Migraine is an incapacitating pain disorder, which manifests in attacks of often unilateral headache accompanied by photophobia, phonophobia, and nausea. Cerebrovascular changes, particularly those associated with the large veins and sinuses, have been considered the foundation of migraine pathophysiology for some time. This peripheral sensitization theory is based on the notion that migraines are triggered by sensitization of meningeal nociceptors that evoke activation of trigemino-vascular neurons resulting in throbbing head pain and other migraine symptoms (Borsook & Burstein, 2012; Bernstein & Burstein, 2012). While the idea that a peripheral trigger is critical for the generation of migraine is well-accepted, there is growing evidence that changes in the central nervous system may also play a critical role (Akerman,

Holland, & Goadsby, 2011; Goadsby, 2009; Goadsby, Charbit, Andreou, Akerman, & Holland, 2009). Such evidence includes observations that symptoms such as fatigue, dizziness, and reduced concentration occur hours before the migraine onset (Giffin et al., 2003) and that activation of brainstem trigemino-vascular neurons by cortical spreading depression can occur independently of peripheral input (Lambert, Truong, & Zagami, 2011). Indeed, it was recently proposed that migraine results from dysfunction in subcortical sites which results in the perception of pain from “basal levels of primary traffic” (Goadsby & Akerman, 2012). This “central generator” theory is hotly debated with many researchers suggesting that a peripheral cerebrovascular trigger is necessary to precipitate a migraine attack (Borsook & Burstein, 2012).

However, even if a peripheral cerebrovascular trigger is required, sensitivity changes in brainstem regions that receive noxious orofacial

inputs may be critical in allowing such a trigger to evoke a migraine attack. Consistent with this idea, it has been hypothesized that in migraineurs, brainstem function oscillates between (a) enhanced, (b) threshold, and (c) diminished neural “tone” states (Burststein, Nosedá, & Borsook, 2015). When the brainstem is in a state of *diminished tone*, incoming noxious inputs can activate central pathways and evoke head pain. In contrast, when in an enhanced tone state, the effectiveness of endogenous analgesic mechanisms is too great to allow incoming noxious inputs to activate higher brain centers and head pain does not occur. Although *during* spontaneous or triggered migraine attacks, regional brainstem and hypothalamic activation occurs (Afridi et al., 2005a, 2005b; Bahra, Matharu, Buchel, Frackowiak, & Goadsby, 2001; Denuelle, Fabre, Payoux, Chollet, & Geraud, 2007; Weiller et al., 1995), there is currently little evidence to support the notion of cyclical changes in brainstem and/or hypothalamic function throughout the migraine cycle, particularly in the hours preceding a migraine headache. Some support comes from a recent case study which reported that the hypothalamus displayed increased sensitivity to noxious stimuli and greater functional coupling with the dorsomedial pons and spinal trigeminal nucleus (SpV) during the phase immediately prior to an attack (Schulte & May, 2016).

In individuals who experience migraine with aura, cortical spreading depression precedes the development of head pain. This phenomenon is characterized by a wave of electrophysiological hyperactivity followed by inhibition and there is evidence that this process is associated with astrocyte calcium waves (James, Smith, Boniface, Huang, & Leslie, 2001; Nedergaard, Cooper, & Goldman, 1995). These calcium waves are linked to gliotransmitter release and it has been proposed that in some pathological cases, greater numbers of astrocytes may display enhanced calcium wave synchrony and amplitude and this results in significantly altered synaptic function (Halassa, Fellin, & Haydon, 2007; Parri, Gould, & Crunelli, 2001). It is possible that altered brainstem *tone* during the migraine cycle results from synaptic activity modulated by changes in gliotransmission. Indeed, we recently reported that chronic neuropathic head pain is *not* associated with increased activity but rather with increased resting oscillations in the infra-slow range in the ascending trigeminal pathway, a frequency range remarkably similar to that of rhythmic gliotransmitter release (0.03–0.06 Hz) (Alshelh et al., 2016). Infra-slow oscillatory activity is a fundamental property of cerebral and thalamic function and is thought to be maintained by adenosine receptor-mediated signaling (Hughes, Lorincz, Parri, & Crunelli, 2011; Lorincz, Geall, Bao, Crunelli, & Hughes, 2009). This adenosine is likely released by astrocytes since they can display spontaneous intracellular infra-slow calcium oscillations and are responsive to glutamate and acetylcholine (Parri & Crunelli, 2001), and a link between adenosine and infra-slow oscillatory cortex activity has been demonstrated (Cunningham et al., 2006). Given this, we hypothesize that increased oscillatory gliotransmitter release in brainstem regions that regulate activity within the ascending trigeminal pathway could alter the propensity for an external noxious input to evoke a migraine attack.

The aim of this investigation is to determine if ongoing activity patterns, as reflected in infra-slow oscillations and functional connectivity

within the brainstem and hypothalamus, are altered over the migraine cycle and in particular directly prior to a migraine headache. We hypothesize that infra-slow oscillatory activity and functional connectivity within the brainstem and hypothalamus will increase significantly directly *prior* to a migraine headache and then return to control levels following the migraine headache. Furthermore, since in pathological conditions greater numbers of astrocytes may display enhanced calcium wave synchrony and amplitude, we speculate that immediately prior to a migraine attack, greater activity synchronization between adjacent voxels, that is greater regional homogeneity, will occur within brainstem and hypothalamic sites.

## 2 | METHODS

### 2.1 | Subjects

Twenty-six subjects with migraine (22 females; mean age  $30.6 \pm 2.1$  years [ $\pm$ SEM]) and 78 pain-free controls (66 females; mean age  $30.7 \pm 1.3$  years) were recruited for the study from the general population using an advertisement. There were no significant differences in age ( $t$  test;  $p > .05$ ) or gender composition (chi-squared test,  $p > .05$ ) between the two subject groups. Migraine subjects were diagnosed according to the IHC Classification ICHD-3 BETA criteria and five of the 26 migraine subjects reported an aura associated with their migraine attacks. Migraine subject characteristics, including medication use are shown in Table 1. All migraineurs were scanned during an interictal period, that is, at least 72 h after and 24 h prior to a migraine event. Eleven of these migraineurs were also scanned immediately (within 72 h) following an attack and eight immediately (within 24 h) prior to an attack. It is important to note that of the subjects scanned immediately prior to an attack, there was no predicting factor that they were within 24 h of a migraine. In five migraineurs, scans were collected during all three phases (interictal, immediately prior to and immediately following an attack). Exclusion criteria for controls were the presence of any pain condition including family history of migraines, current use of analgesics, or any neurological disorder. Exclusion criteria for migraineurs were any other pain condition or neurological disorder. No migraineur was excluded based on their medication use and no migraine or control subject had an incidental neurological finding that resulted in their exclusion from the study. All migraineurs indicated the intensity (6-point visual analogue scale; 0 = no pain, 5 = most intense imaginable pain) and drew the facial distribution of pain commonly experienced during a migraine attack. In addition, each subject described the qualities of their migraines and indicated any current treatments used to prevent or abort a migraine once started. Twenty-five of the 26 migraineurs had episodic migraine whereas the remaining migraineur had chronic migraine ( $>15$  migraines per month). Informed written consent was obtained for all procedures according to the Declaration of Helsinki and local Institutional Human Research Ethics Committees approved the study. Data from 25 of the 26 migraineurs and 30 of the control subjects were used in a previous investigation (Marciszewski et al., 2017).

TABLE 1 Migraine subject characteristics

Subject	Age	Sex	Years suffering	Pain side	Aura	Migraines, months	Intensity (0–5)	Medication taken during migraine	Daily medication
270	31	F	25	R	Y	5–8	3–4	Paracetamol	-
500	55	M	15	B	N	15 (chronic)	3	Paracetamol	-
548	24	F	20	B	N	4	4	Ibuprofen, paracetamol	OCP, budesonide/formoterol
583	26	F	12	R	N	2	3–4	Ibuprofen	OCP
661	27	F	12	R	Y	1	4	Ibuprofen	OCP
664	23	F	4	R	N	4	4	Triptan	OCP, metformin hydrochloride
666	25	F	12	L	N	5	3	Aspirin, rizatriptan	Desvenlafaxine
668	21	F	1.5	L	N	4	3	Ibuprofen, paracetamol, codeine	OCP
670	26	F	1	L	N	3	5	Paracetamol	OCP
671	29	F	13	R	N	1	2.5	Ibuprofen	Zopiclone
672	26	F	5	R	N	1	2	Aspirin, codeine, ibuprofen	OCP
676	23	F	6	R	N	1	3–4	Ibuprofen	OCP
677	23	F	10	B	N	0.5–1	4	Ibuprofen, codeine	OCP
678	46	F	15–20	B	N	1	3	Sumatriptan	-
679	41	F	40	B	N	2	4	Sumatriptan	-
681	23	M	3–4	B	N	0.5–1	3.5	Paracetamol, codeine	-
688	23	M	4–5	B	N	0.5–1	4	Paracetamol	-
696	55	F	40	R	N	0.5–1	3–4	Sumatriptan	Telmisartan
800	26	M	20	R	N	0.5–1	4	Metamizole	Carbamazepine
814	49	F	30	B	N	0.5–1	5	Rizatriptan, paracetamol	-
815	54	F	30	B	N	0.5–1	5	Paracetamol, codeine, eletriptan,	Candesartan
818	34	F	15	L	Y	2	3	Paracetamol, ibuprofen	-
819	26	F	5	B	Y	1	3	Paracetamol	OCP
820	25	F	7–8	L	N	5–8	3	Rizatriptan benzoate	OCP
822	27	M	4	B	N	0.5–1	4	Ibuprofen	SSRI
825	28	F	25	R	Y	0.25	5	Ibuprofen	Methylphenidate

Note. Abbreviations: B = bilateral; L = left; OCP = oral contraceptive pill; R = right; SSRI = selective serotonin reuptake inhibitor.

## 2.2 | MRI acquisition

All subjects lay supine on the bed of a 3 T MRI scanner (Philips, Achieva) with their head immobilized in a tight-fitting head coil. With each subject relaxed and at rest, a high-resolution 3D T1-weighted anatomical image set, covering the entire brain, was collected (turbo field echo; field of view = 250 × 250 mm, matrix size = 288 × 288, slice thickness = 0.87 mm, repetition time = 5,600 ms; echo time = 2.5 ms, flip angle = 8°). Following this, a series of 180 gradient echo echo-planar functional MRI image volumes using blood oxygen level dependent (BOLD) contrast were collected. Each image volume contained 35 axial slices covering the entire brain (field of view = 240 × 240 mm, matrix size = 80 × 78,

slice thickness = 4 mm, repetition time = 2,000 ms; echo time = 30 ms, flip angle = 90°).

## 2.3 | MRI processing and statistical analysis

### 2.3.1 | Image preprocessing

Using SPM12 and Matlab software, all fMRI images were motion corrected and detrended to remove global signal drifts (Macey, Macey, Kumar, & Harper, 2004). In no subject was there significant movement (>0.5 mm in any direction) and all subjects were used for the subsequent analysis. In five migraineurs who experienced migraines most often on the left side, their images were reflected in the X plane ("flipped") so that fMRI signals could be assessed ipsilateral and

contralateral to the most common side of migraine. Each subject's fMRI image set was coregistered to their own T1-weighted anatomical image set. The T1 images were then spatially normalized to the Montreal Neurological Institute (MNI) template and the parameters applied to the fMRI image sets so that both the T1-weighted and fMRI images were in the same locations in three-dimensional space. To remove the potential influence of signal intensity changes within the cerebrospinal fluid, cerebrospinal fluid brain maps were created by segmenting the spatially normalized T1 anatomical images. This map was used to mask the fMRI images so that only grey and white matter remained. In all subsequent analyses, the anatomical locations of significant clusters were confirmed using the Atlas of the Human Brain by Mai, Paxinos, and Voss (2007) and the Atlas of the Human Brainstem by Paxinos and Huang (1995).

### 2.3.2 | Infra-slow oscillation power

Using the SPM DPARSF toolbox, raw power between 0.03 and 0.06 Hz was calculated for each voxel of the unsmoothed fMRI image sets in the control subjects, and in the migraine subjects during the interictal phase, and the phases immediately prior to and immediately following an attack. The resulting brain maps were then smoothed using a 3 mm full-width-half-maximum Gaussian filter. A small smoothing kernel was chosen to maintain spatial accuracy as we hypothesized that we would find differences in small brainstem and diencephalic structures. Three whole brain voxel-by-voxel comparisons were then performed: (a) controls ( $n = 78$ ) compared with migraineurs during their interictal phase ( $n = 26$ ), (b) controls ( $n = 78$ ) compared with migraineurs during the phase immediately prior to a migraine ( $n = 8$ ), and (c) controls ( $n = 78$ ) compared with migraineurs during the phase immediately following an attack ( $n = 11$ ). Significant differences were determined using two-sample random effects procedures with age and gender as nuisance variables ( $p < .05$ , false discovery rate corrected, minimum cluster size 5 voxels). Significant power differences compared with controls, occurred in migraineurs immediately prior to an attack only and the power values from these significant clusters were determined for controls and migraineurs during all three phases. For one large cluster that encompassed the hypothalamus, periaqueductal gray (PAG), and dorsomedial medulla, secondary peaks within the cluster were selected and the power values of these regions (10 most significant voxels around the peak) were extracted. Significant differences in these extracted power values between subjects scanned in interictal, immediately prior to and immediately following an attack were determined ( $p < .05$ , two-tailed, two-sample  $t$  test, Bonferroni corrected for multiple comparisons). Differences between controls and migraineurs were not assessed in the cluster analysis as these comparisons were performed in the initial voxel-by-voxel whole-brain analyses. To explore individual subject changes, raw power values from significant clusters were plotted in the five migraineurs in whom we collected fMRI scans during all three phases.

We also divided these raw power values by the total power over the entire frequency range to obtain fractional power value for each voxel. The mean fractional powers were also calculated for each significant cluster and significant differences between controls and subjects scanned in interictal, immediately prior to and immediately following an

attack were determined ( $p < .05$ , two-tailed, two-sample  $t$  test, Bonferroni corrected for multiple comparisons). For each significant cluster, we also calculated ALFF power for the four most commonly used infra-slow oscillatory frequency bands, slow 2: 0.198–0.25 Hz, slow 3: 0.073–0.198 Hz, slow 4: 0.027–0.073 Hz, and slow 5: 0.01–0.027 Hz). Significant differences between controls and subjects scanned in interictal, immediately prior to and immediately following an attack were then determined for each of these infra-slow oscillatory frequency bands ( $p < .05$ , two-tailed, two-sample  $t$  test, Bonferroni corrected for multiple comparisons).

### 2.3.3 | Regional homogeneity

To assess regional homogeneity, the similarity of the time series within each voxel and its 7 nearest neighbors were measured by calculating Kendall's coefficient of concordance. Using the unsmoothed fMRI image sets, subject-level Z-score maps were created by subtracting the mean Kendall's coefficient of concordance for the entire brain from each voxel and dividing by the mean standard deviation. The resulting brain maps were then smoothed using a 3 mm full-width-half-maximum Gaussian filter. Significant differences in regional homogeneity between controls and migraineurs immediately prior to an attack were then determined using a two-sample random effects procedure with age and gender as nuisance variables ( $p < .05$ , false discovery rate corrected, minimum cluster size 5 voxels). In addition, regional homogeneity values were extracted for each significant cluster and plotted for controls and migraineurs during all three phases and significant differences between controls, and subjects scanned in interictal, immediately prior to and immediately following an attack were determined ( $p < .05$ , two-tailed, two-sample  $t$  test, Bonferroni corrected for multiple comparisons). Differences between controls and migraineurs scanned immediately prior to an attack were not assessed as these comparisons were performed in the voxel-by-voxel whole-brain analysis. Regional homogeneity values from the significant clusters were also plotted in the five migraineurs in which we collected fMRI scans during all three phases.

### 2.3.4 | Functional connectivity

Finally, resting functional connectivity was assessed in controls and migraineurs using a seed located in the midbrain PAG. This seed was derived from the overlap between increased infra-slow oscillation power and regional homogeneity in migraineurs immediately prior to an attack. Mean resting signal intensity changes within this seed were calculated and a voxel-by-voxel analysis was performed to determine areas that displayed significant signal intensity covariations with the seed signal. In each subject, the 6 direction movement parameters calculated during the realignment step were included as nuisance variables. The resulting brain maps were then smoothed using a 3 mm full-width-half-maximum Gaussian filter. Significant differences in functional connectivity strengths between controls and migraineurs immediately prior to an attack were then determined using a two-sample random effects procedure with age and gender as nuisance variables ( $p < .05$ , false discovery rate corrected, minimum cluster size 5 voxels). In addition, connectivity strength values were extracted for each significant cluster and plotted for controls and

migraineurs during all three phases and significant differences between controls, and subjects scanned in interictal, immediately prior to and immediately following an attack were determined ( $p < .05$ , two-tailed, two-sample  $t$  test, Bonferroni corrected for multiple comparisons). Differences between controls and migraineurs scanned immediately prior to an attack were not assessed as these comparisons were performed in the voxel-by-voxel whole-brain analysis. Connectivity values from the significant clusters were also plotted in the five migraineurs in whom we collected fMRI scans during all three phases.

## 3 | RESULTS

### 3.1 | Infra-slow oscillations

Infra-slow oscillations were measured at rest using fMRI in 78 healthy controls and 26 migraineurs. Eight of the migraineurs were scanned immediately prior to an attack (within 24 h), 11 were scanned immediately following an attack (within 72 h) and all 26 migraineurs were scanned during the interictal phase (more than 24 h before the next migraine, and more than 72 h after a migraine).

We first compared resting fMRI signals throughout the entire brain in migraineurs during all three phases (interictal, immediately prior to and immediately following an attack) with resting fMRI signals in controls. Fast Fourier Transforms of resting fMRI signal intensity fluctuations were performed and the mean power between 0.03 and 0.06 Hz determined for each voxel in each subject. Comparison of power between controls and migraineurs in each voxel revealed a striking pattern of increased infra-slow oscillatory power in migraineurs *only* in the phase immediately prior to an attack (Figure 1a and Table 2). This increased infra-slow oscillatory power during the phase immediately prior to an attack was almost entirely restricted to the brainstem, hypothalamus, and thalamus. During the phase immediately prior to an attack, increased oscillatory power occurred in the region of the right (ipsilateral to side of most frequent migraine) spinal trigeminal nucleus (SpV) extending into the rostral ventromedial medulla (RVM), dorsomedial pons, midbrain in the region of the PAG, posterior hypothalamus, and in the thalamus in the region of the somatosensory nucleus (Figure 1b). In no brain region was infra-slow oscillatory power reduced in migraineurs compared with controls.

Plots of raw power extracted from these regions in controls and migraineurs during all three phases confirmed the specificity of power increases during the phase immediately prior to an attack only in the SpV/RVM (mean  $\pm$  SEM 0.03–0.06 Hz power: controls:  $1.04 \pm 0.03$ , interictal:  $1.19 \pm 0.06$ , immediately prior to an attack:  $1.54 \pm 0.13$ , immediately following an attack:  $1.02 \pm 0.02$ ), dorsomedial pons (controls:  $1.01 \pm 0.03$ , interictal:  $1.06 \pm 0.04$ , immediately prior to an attack:  $1.55 \pm 0.19$ , immediately following an attack:  $1.03 \pm 0.01$ ), PAG (controls:  $1.05 \pm 0.03$ , interictal:  $1.08 \pm 0.05$ , immediately prior to an attack:  $1.59 \pm 0.19$ , immediately following an attack:  $1.03 \pm 0.02$ ) hypothalamus (controls:  $1.17 \pm 0.03$ , interictal:  $1.24 \pm 0.05$ , immediately prior to an attack:  $1.68 \pm 0.17$ , immediately following an attack:  $1.17 \pm 0.03$ ) and somatosensory thalamus (controls:  $0.99 \pm 0.02$ , interictal:  $1.04 \pm 0.05$ , immediately prior to an attack:  $1.32 \pm 0.12$ ,

immediately following an attack:  $1.02 \pm 0.02$ ) (Figure 1c). In addition to the significant power increases in migraineurs in the phase immediately prior to an attack compared with controls, comparison of power values within the migraineurs group revealed significant differences between the phase immediately prior to an attack and the interictal phase in the dorsomedial pons, PAG, and hypothalamus and a significant difference between the phases immediately prior to and following an attack in the SpV/RVM, dorsomedial pons, and PAG.

As raw power can be influenced by an individual's global infra-slow oscillatory power, we also calculated fractional power by dividing the raw 0.03–0.06 Hz power at each voxel by the total power over the entire frequency range (0–0.25 Hz). For each of the significant clusters derived from the raw power analysis, we found significantly increased fractional power during only the phase immediately prior to an attack compared with controls. These fractional power increases occurred in the SpV (mean  $\pm$  SEM: controls:  $0.76 \pm 0.01$ , interictal:  $0.81 \pm 0.02$ , immediately prior to an attack:  $0.87 \pm 0.04$ , immediately following an attack:  $0.78 \pm 0.01$ ), dorsomedial pons (controls:  $0.91 \pm 0.01$ , interictal:  $0.93 \pm 0.01$ , immediately prior to an attack:  $1.00 \pm 0.02$ , immediately following an attack:  $0.91 \pm 0.01$ ), PAG (controls:  $0.78 \pm 0.01$ , interictal:  $0.83 \pm 0.03$ , immediately prior to an attack:  $0.89 \pm 0.05$ , immediately following an attack:  $0.80 \pm 0.01$ ) and hypothalamus (controls:  $0.84 \pm 0.01$ , interictal:  $0.87 \pm 0.02$ , immediately prior to an attack:  $0.93 \pm 0.04$ , immediately following an attack:  $0.83 \pm 0.01$ ). No significant differences in fractional power occurred in the somatosensory thalamus (controls:  $0.95 \pm 0.01$ , interictal:  $0.96 \pm 0.03$ , immediately prior to an attack:  $0.98 \pm 0.04$ , immediately following an attack:  $0.94 \pm 0.01$ ).

Assessments of four infra-slow oscillatory bands revealed an interesting frequency specificity (Figure 1d). While there were no significant differences in infra-slow oscillatory power during any migraine phase and controls for the SpV, in contrast the PAG and hypothalamus displayed greater power for band 4 (0.27–0.71 Hz) only in the phase immediately prior to the migraine compared with controls. This band includes the infra-slow oscillatory band specifically investigated in this study (0.03–0.06 Hz). Furthermore, for the dorsomedial pons and thalamus, power was significantly greater during the phase immediately prior to the migraine attack compared with controls for all four infra-slow oscillatory bands, suggestive of a more widespread increase in infra-slow oscillatory power.

### 3.2 | Regional homogeneity

If increased infra-slow oscillation power during the phase immediately prior to an attack is associated with increased synchronicity of astrocyte activation and the subsequent recruitment of surrounding astrocytes and neurons, neighboring voxels should display increased signal intensity synchronization. To determine if there was such an increase in regional homogeneity, we measured Kendall's coefficient of concordance (KCC) to evaluate the similarity of the time series within each voxel to its seven nearest neighbors, in controls and migraineurs. Comparison of regional homogeneity between migraineurs and controls at each voxel in the brain revealed a significant increase during the phase immediately prior to an attack but no significant differences between

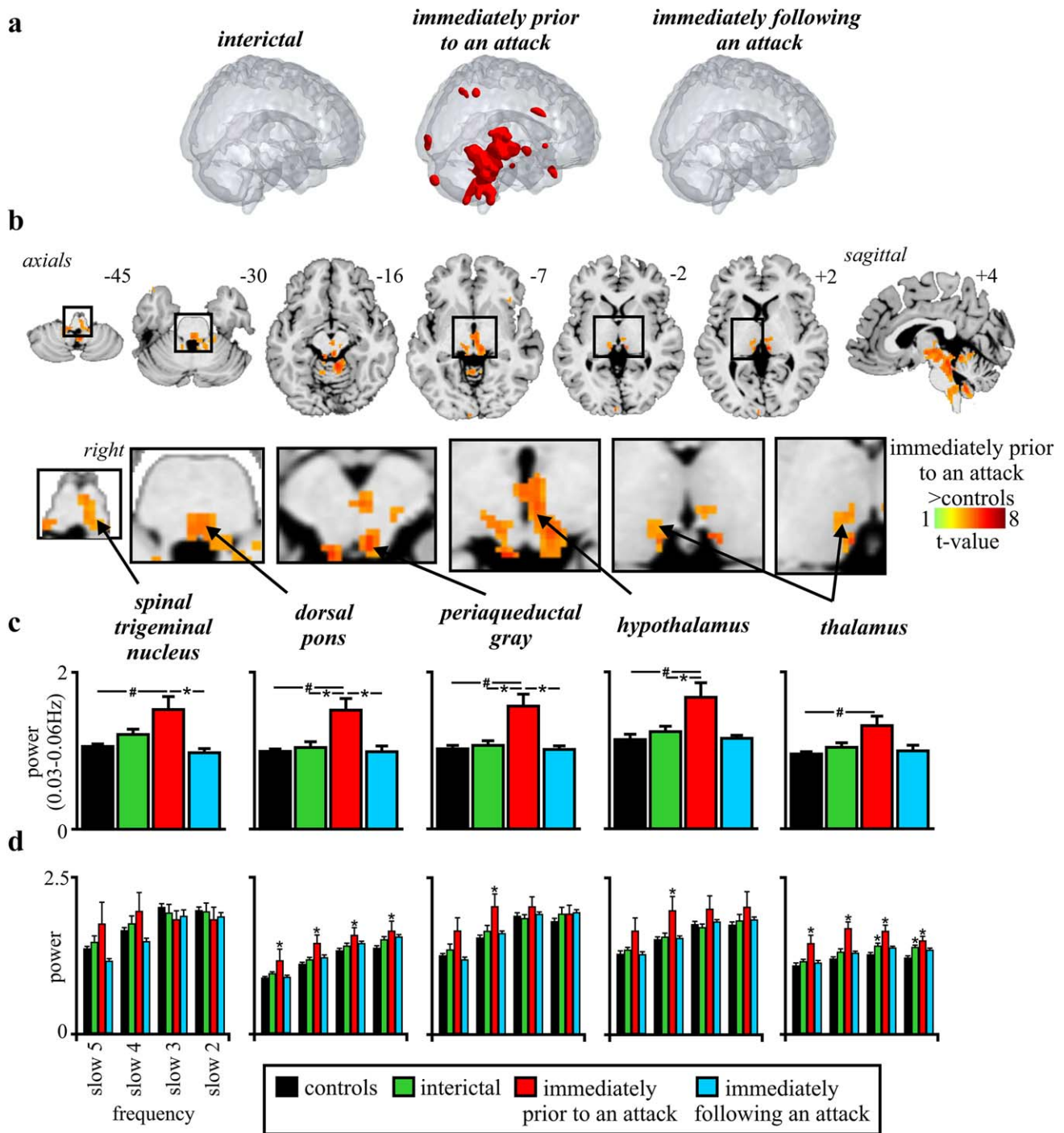


**FIGURE 1** (a) Significant differences in infra-slow oscillation power between controls ( $n = 78$ ) and migraineurs during interictal phase ( $n = 26$ ), immediately prior to an attack ( $n = 8$ ) and immediately following an attack ( $n = 11$ ). Note that only during the phase immediately prior to an attack was power significantly different to controls and this difference occurred primarily in the brainstem and hypothalamus. (b) Brain regions in which infra-slow oscillation power was greater in migraineurs immediately prior to a migraine compared with controls (random effects,  $p < .05$ , false discovery rate corrected). Location of each axial slice in Montreal Neurological Institute space is indicated at the top right. (c) Plots of mean ( $\pm$ SEM) power between 0.03 and 0.06 Hz in significant clusters extracted from controls and migraineurs during all three phases. In addition to significant power increases in all clusters during the phase immediately prior to an attack compared with controls ( $\#p < .05$  derived from random effects whole-brain analysis), there were significant differences between the phase immediately prior to an attack and the interictal phase in all clusters except for the thalamus ( $*p < .05$  derived from post-hoc two-sample  $t$  test). (d) Plots of mean ( $\pm$ SEM) power over four standard infra-slow frequency bands: slow 2: 0.027–0.073 Hz, slow 3: 0.073–0.198 Hz, slow 4: 0.027–0.073 Hz, and slow 5: 0.01–0.027 Hz ( $*p < .05$  significantly different to controls derived from post-hoc two-sample  $t$  test)

**TABLE 2** Montreal Neurological Institute (MNI) coordinates, cluster size, and *t* score for regions of significant difference between control and migraineurs during the phase immediately prior to an attack

(a) Brain region	(b) MNI co-ordinate			Cluster size	t score
	x	y	z		
<i>Infra-slow oscillation power (0.03–0.06 Hz)</i>					
Immediately prior to an attack > controls					
Dorsal pons	8	–40	–24	817	5.47
Hypothalamus	0	–16	–10	59	5.31
Midbrain periaqueductal gray	4	–32	–18	228	5.29
Dorsomedial pons	–4	–38	–36		4.34
Spinal trigeminal nucleus/rostral ventromedial medulla	4	–34	–46		4.03
Thalamus	–6	–26	10		5.51
<i>Regional homogeneity</i>					
Immediately prior to an attack > controls					
midbrain periaqueductal gray	–4	–28	–8	42	4.36
Hypothalamus	2	–12	–12	6	4.64
Thalamus	–12	–24	2	10	4.18
<i>Resting functional connectivity</i>					
Immediately prior to an attack > controls					
Midbrain periaqueductal gray	4	–34	–18	7	4.82
Hypothalamus	0	–16	–10	23	4.86
Thalamus	–10	–24	–2	8	4.32

migraineurs and controls during either the interictal phase or the phase immediately following an attack. During the phase immediately prior to an attack, migraineurs had significantly increased regional homogeneity restricted almost entirely to regions of the PAG, hypothalamus, and somatosensory thalamus (Figure 2a and Table 2). In no brain region was regional homogeneity significantly lower in migraineurs than in controls.

Plots of regional homogeneity extracted from these regions in controls and migraineurs during all three phases revealed regional homogeneity increases during only the phase directly prior to an attack in the PAG (mean  $\pm$  SEM KCC: controls:  $0.44 \pm 0.01$ , interictal:  $0.46 \pm 0.01$ , immediately prior to an attack:  $0.54 \pm 0.03$ , immediately following an attack:  $0.44 \pm 0.05$ ) and thalamus (controls:  $0.92 \pm 0.01$ , interictal:  $0.97 \pm 0.02$ , immediately prior to an attack:  $1.09 \pm 0.03$ , immediately following an attack:  $0.94 \pm 0.01$ ) and increases during both the interictal phase and the phase immediately prior to an attack compared with controls in the hypothalamus (controls:  $0.97 \pm 0.01$ , interictal:  $1.03 \pm 0.02$ , immediately prior to an attack:  $1.11 \pm 0.04$ , immediately following an attack:  $0.99 \pm 0.01$ ). The PAG, hypothalamus, and thalamus all showed increases in both infra-slow oscillatory power and regional homogeneity in migraineurs during the phase immediately prior to an attack, compared with controls (Figure 2b). We also extracted these values from clusters derived from the infra-slow oscillation analysis, to confirm that there were no changes in regional homogeneity in the SpV/RVM (controls:  $0.94 \pm 0.01$ , interictal:  $0.98 \pm 0.02$ , immediately

prior to an attack:  $0.99 \pm 0.03$ , immediately following an attack:  $0.99 \pm 0.02$ , all  $p > .05$ ) or dorsomedial pons (controls:  $0.93 \pm 0.01$ , interictal:  $0.94 \pm 0.01$ , immediately prior to an attack:  $0.97 \pm 0.03$ , immediately following an attack:  $0.95 \pm 0.02$ , all  $p > .05$ ).

### 3.3 | Periaqueductal gray matter connectivity

Given previous reports of altered connectivity between the diencephalon and brainstem in migraineurs, we assessed resting functional connectivity changes using the PAG as a seed. Comparison of PAG connectivity in the phase immediately prior to an attack in migraineurs with that of controls revealed significant increases in functional connectivity strength between the PAG and the hypothalamus, thalamus and between the rostral and caudal regions of the PAG matter (Figure 3 and Table 2). In no region was connectivity strength significantly lower in migraineurs compared with controls. Plots of connectivity strengths extracted from these regions in controls and migraineurs during all three phases revealed a consistent pattern of difference; all three regions showed significantly greater connectivity strengths during the phase immediately prior to an attack than in the interictal phase and in the phase immediately following an attack in migraineurs, and compared with controls: PAG (mean  $\pm$  SEM connectivity strength: controls:  $0.34 \pm 0.03$ , interictal:  $0.23 \pm 0.07$ , immediately prior to an attack:  $0.76 \pm 0.13$ , immediately following an attack:  $0.36 \pm 0.02$ ), hypothalamus (controls:  $0.34 \pm 0.05$ ,



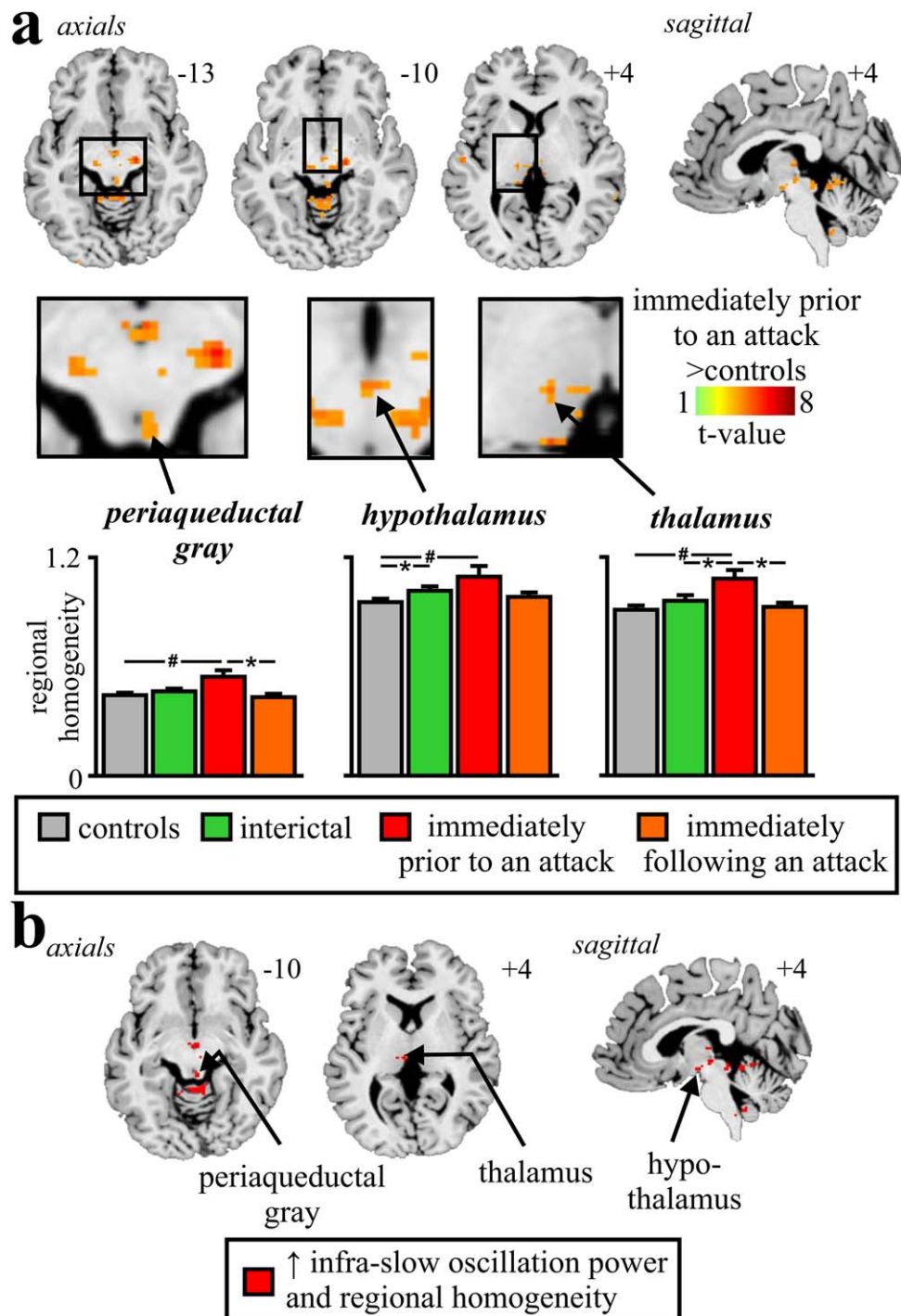


**FIGURE 2** (a) Brain regions in which regional homogeneity was significantly different between controls ( $n = 78$ ) and migraineurs during the phase immediately prior to an attack ( $n = 8$ ). Location of each axial slice in Montreal Neurological Institute space is indicated at the top right. Significant increases in regional homogeneity occurred in the rostral brainstem, hypothalamus, and thalamus. Below are plots of mean ( $\pm$ SEM) regional homogeneity in significant clusters extracted from controls and migraineurs during all three phases. In addition to significant power increases in all clusters during the phase immediately prior to an attack compared with controls ( $^{\#}p < .05$  derived from random effects whole-brain analysis), there were significant differences between the phases immediately prior to, and following an attack ( $n = 11$ ) in the PAG and between controls and interictal phase in migraineurs ( $n = 26$ ), in the hypothalamus ( $^*p < .05$  derived from post-hoc two-sample  $t$  test). (b) Brain regions in which during the phase immediately prior to an attack, migraineurs displayed greater infra-slow oscillation power and regional homogeneity compared with controls

interictal:  $0.36 \pm 0.09$ , immediately prior to an attack:  $1.01 \pm 0.12$ , immediately following an attack:  $0.58 \pm 0.05$  and thalamus (controls:  $0.19 \pm 0.03$ , interictal:  $0.24 \pm 0.04$ , immediately prior to an attack:

$0.57 \pm 0.08$ , immediately following an attack:  $0.24 \pm 0.02$ ). To ensure that there was indeed no change in resting functional connectivity between the PAG and/or dorsomedial pons SpV/RVM we extracted

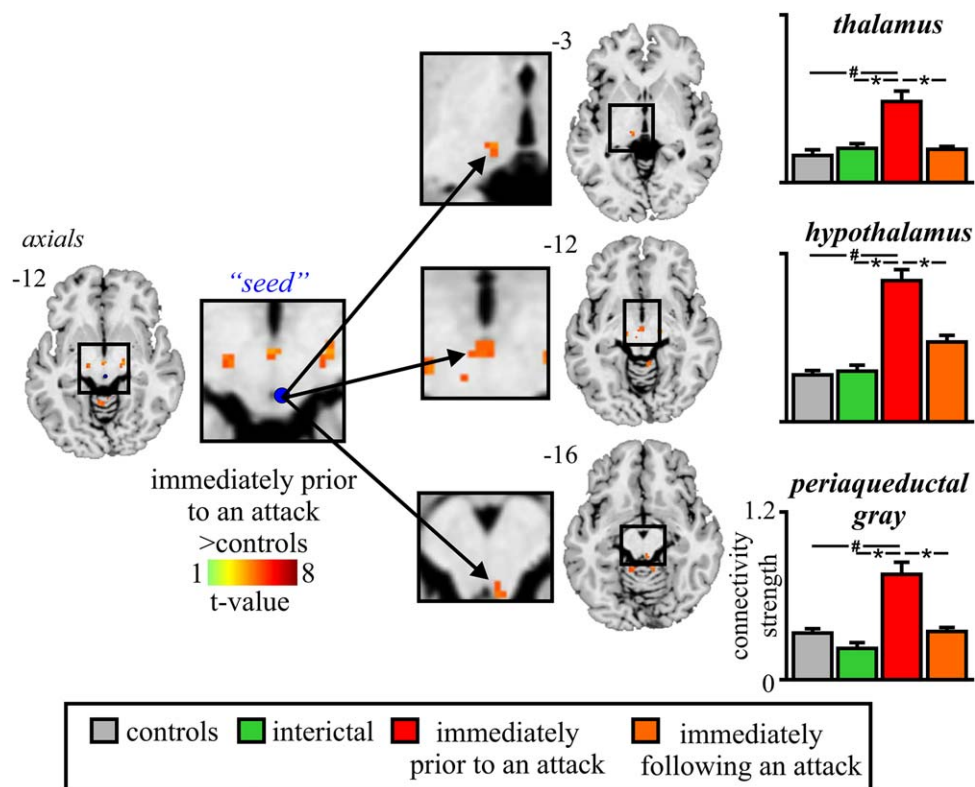


**FIGURE 3** Brain regions in which resting functional connectivity was significantly different between controls ( $n = 78$ ) and migraineurs during the phase immediately prior to an attack ( $n = 8$ ). Location of each axial slice in Montreal Neurological Institute space is indicated at the top right. Significant increases in resting connectivity occurred in migraineurs between the PAG and the thalamus, hypothalamus, and between the rostral and caudal PAG. To the right are plots of mean ( $\pm$ SEM) connectivity strength in significant clusters extracted from controls and migraineurs during all three phases. In addition to significant increases in connectivity strength in all clusters during the phases immediately prior to, and following an attack ( $n = 11$ ) in migraineurs compared with controls ( $^{\#}p < .05$  derived from random effects whole-brain analysis), there were significant differences between the phases immediately prior to and following an attack in the PAG and between controls and interictal phase in the hypothalamus.  $^{\#}p < .05$  derived from random effects whole-brain analysis ( $^*p < .05$  derived from post-hoc two-sample  $t$  test)

values from these regions and found no significant PAG connectivity with the SpV/RVM (controls:  $-0.02 \pm 0.02$ , interictal:  $-0.13 \pm 0.11$ , immediately prior to an attack:  $-0.08 \pm 0.08$ , immediately following an attack:  $0.01 \pm 0.08$ , all  $p > .05$ ) or dorsomedial pons (controls:  $0.15 \pm 0.02$ , interictal:  $0.19 \pm 0.07$ , immediately prior to an attack:  $0.33 \pm 0.12$ , immediately following an attack:  $0.09 \pm 0.07$ , all  $p > .05$ ).

### 3.4 | Individual subject changes

In five migraineurs, resting fMRI scans were collected during all three phases, that is, interictal, the phases immediately prior to and following an attack. To explore individual variations, we plotted infra-slow oscillatory power, regional homogeneity, and connectivity for each subject during each migraine phase. These plots reveal a remarkably consistent pattern of changes with greater infra-slow oscillatory power (Figure 4a), increased regional homogeneity (Figure 4b), and greater functional connectivity strength (Figure 4c) during the phase immediately prior to an attack compared with the interictal and the phase immediately following an attack.

## 4 | DISCUSSION

We describe here a series of experimental findings revealing altered brainstem and hypothalamic function in the period immediately prior to a migraine headache. These changes include increases in infra-slow oscillatory activity, hypothalamic-brainstem functional connectivity, and regional homogeneity. Importantly, these oscillatory and network alterations only occur directly prior to a migraine headache, while the individual is not in pain, and do not occur during other migraine phases. While these results do not provide direct evidence that changes in these brain regions are subsequently responsible for the initiation of a migraine attack, they clearly show that brain activity pattern changes occur immediately prior to a migraine attack while the individual is not in pain. These data are consistent with the idea that changes within the central nervous system are potentially involved in the expression of migraine.

Remarkably, even though we investigated every voxel in the brain during different phases of migraine, only brainstem, hypothalamic, and thalamic regions displayed altered oscillatory activity directly prior to a migraine headache. It is important to emphasize that these alterations

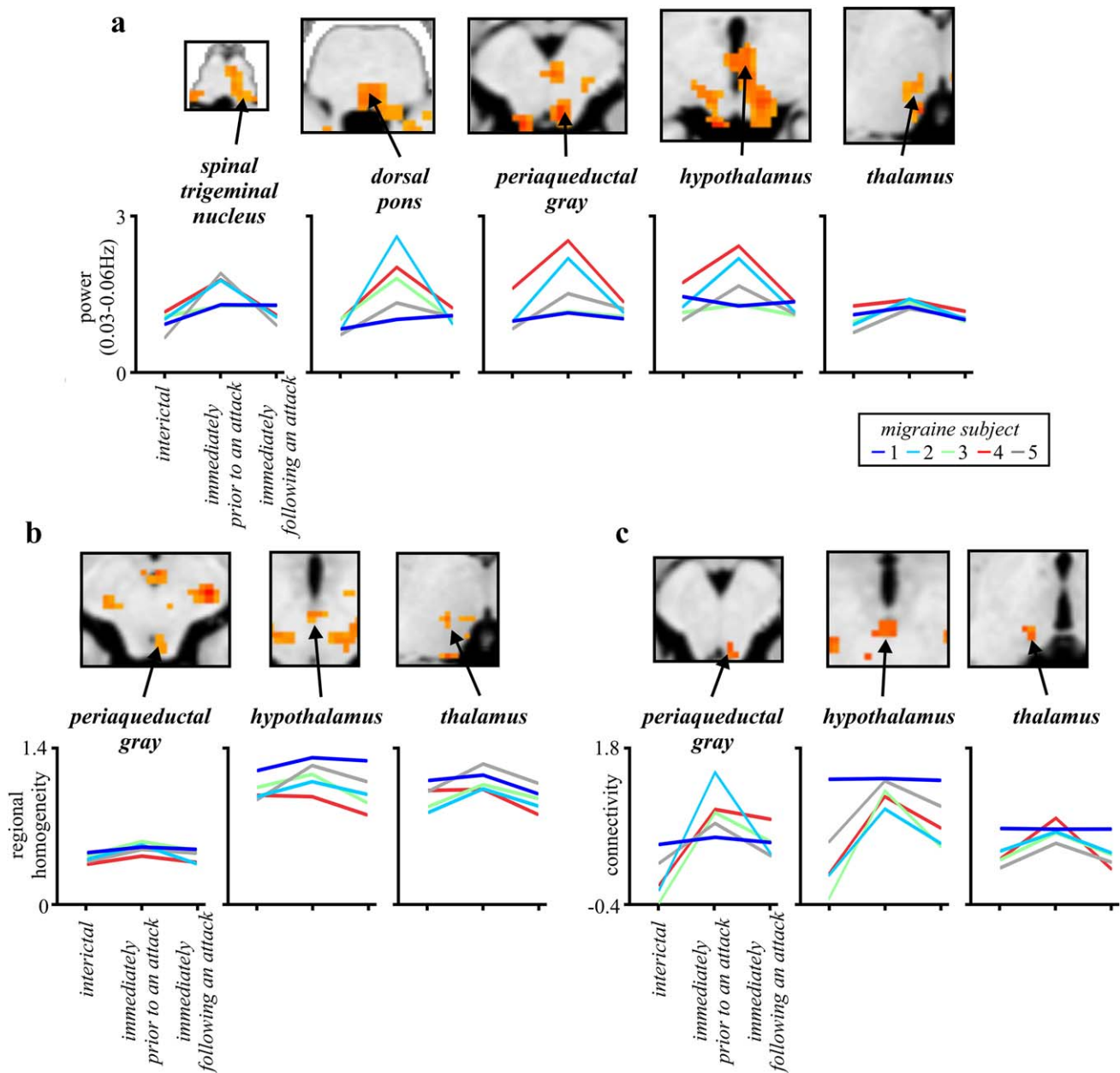


**FIGURE 4** (a) Infra-slow oscillation power, (b) regional homogeneity, and (c) resting functional connectivity in migraineurs ( $n = 5$ ) during the interictal phase, and the phases immediately prior to and following an attack. Values were extracted from clusters derived from whole group analyses. The results indicate that at the individual subject level, the phase immediately prior to an attack is consistently associated with increased infra-slow power, regional homogeneity, and resting connectivity in the brainstem, hypothalamus, and thalamus

were observed while the individual was *not* in pain, that is, was not experiencing a migraine headache. Interestingly, the spatial pattern of this increase in oscillatory power directly prior to a migraine is remarkably similar to that which occurs during a migraine headache itself (Afridi et al., 2005a, 2005b; Bahra et al., 2001; Denuelle et al., 2007; Weiller et al., 1995); that is, the dorsal pons, hypothalamus, and possibly PAG. Recent evidence suggests that infra-slow oscillations are maintained by adenosine receptor-mediated signaling which is itself associated with cyclic gliotransmitter release (Halassa et al., 2007; Parri & Crunelli, 2001). It has been proposed that astrocytes can exhibit pacemaker oscillations at frequencies between 0.03 and 0.06 Hz and

that astrocyte calcium waves can propagate among surrounding astrocytes through gap junction-mediated coupling and/or gliotransmitter release (Cunningham et al., 2006; Lorincz et al., 2009; Parri & Crunelli, 2001). It has been suggested that in pathological cases greater numbers of astrocytes display enhanced calcium-wave synchrony and amplitude and enhanced *N*-methyl-D-aspartate receptor function (Crunelli et al., 2002; Halassa et al., 2007; Parri & Crunelli, 2001). It is possible that the increases in infra-slow oscillatory power and in regional homogeneity within the brainstem and hypothalamus during the phase immediately prior to an attack results from enhanced amplitude and synchrony of oscillatory gliotransmitter release. These infra-slow oscillations are

coupled to high frequency cortical power fluctuations and to the development of paroxysmal events (Hughes et al., 2011; Mantini, Perrucci, Del Gratta, Romani, & Corbetta, 2007; Vanhatalo et al., 2004).

Over the past two decades, numerous studies have focused on the role of the PAG and its output projections in the pathogenesis of migraine. The PAG can alter incoming noxious inputs, and migraine-like episodes can develop following stereotactic placement of electrodes into the PAG (Veloso, Kumar, & Toth, 1998). The PAG is reciprocally connected to the hypothalamus and sends descending projections to the SpV via the RVM (Floyd, Price, Ferry, Keay, & Bandler, 2001; Holstege & Kuypers, 1982; Morgan, Whittier, Hegarty, & Aicher, 2008). Stimulation of the PAG inhibits incoming neural traffic evoked by dural stimulation (Knight & Goadsby, 2001) and it is possible that modulation of the SpV by the PAG results from activation of “on” cells and inhibition of “off” cells within the RVM (Akerman et al., 2011). Although significant activation of the pons, midbrain, and hypothalamus has been shown to occur during migraine headaches, no activation has been shown to occur within the SpV (Afridi et al., 2005a, 2005b; Bahra et al., 2001; Denuelle et al., 2007; Weiller et al., 1995). This lack of activation might be due to the limited spatial resolution of early brain imaging techniques as experimental animal studies clearly show SpV activation during dural stimulation (Strassman, Mason, Moskowitz, & Maciewicz, 1986; Strassman, Mineta, & Vos, 1994). Additionally, consistent with the idea of oscillating brainstem tone, it was recently shown that SpV activity during nociceptive stimulation was enhanced the closer the individual was to their next migraine (Stankewitz, Aderjan, Eippert, & May, 2011). The results are consistent with our findings of altered brainstem activity patterns, specifically in areas regulating noxious trigeminal inputs. The authors also found increased dorsomedial pontine activation to noxious trigeminal stimulation during migraine headaches, further supporting the role of this region in migraine pain.

In support of the theory that infra-slow frequency calcium waves can propagate among neighboring astrocytes, we found that increased regional homogeneity, a measure of neighboring synchronization, occurred in the same regions of the PAG, hypothalamus, and thalamus during *only* the phase immediately prior to an attack. Increases in regional homogeneity did *not* occur in the dorsal pons or medulla, suggesting that the PAG and hypothalamus are critical for the expression of migraine. While there is no direct evidence that migraine is associated with cyclic astrocyte activation, the idea that in some conditions altered astrocyte function can result in altered neural firing has some foundation. Persistent neuropathic pain has been found to be associated with astrocyte activation in the dorsal horn/SpV (Garrison, Dougherty, Kajander, & Carlton, 1991; Okada-Ogawa et al., 2009; Shi, Gelman, Lisinicchia, & Tang, 2012), and with increased infra-slow oscillation power specifically within the trigeminal pathway including the SpV (Alshelh et al., 2016). Furthermore, inhibiting astrocyte activation attenuates and even reverses neuropathic pain markers in experimental animal models (Churi, Abdel-Aleem, Tumber, Scuderi-Porter, & Taylor, 2008; Ji et al., 2013; Morgenweck, Griggs, Donahue, Zadina, & Taylor, 2013). Additionally, there is a large body of evidence, including from postmortem studies, showing that dysfunctional astrocytes are crucial players in epilepsy pathogenesis (Hubbard & Binder, 2016). One of the

more effective migraine prophylactic medications is the anti-convulsant valproic acid (Linde, Mulleners, Chronicle, & McCrory, 2013), whose anti-epileptic action likely occurs through its ability to reduce the capability of astrocytes to transmit calcium signaling (Tian et al., 2005; Wang et al., 2012). Given the episodic nature of both migraine and epilepsy, it might be the case that cyclical regulation of synaptic transmission by astrocytes results in periods of heightened sensitivity that results in increased firing in both conditions. Furthermore, a form of familial hemiplegic migraine (FHM2) is linked to mutations in a gene that encodes part of the sodium–potassium pump; this gene is expressed primarily in neurons in infants and in astrocytes in adulthood. Curiously, in infancy this mutation manifests as epilepsy, presumably due to neuronal hyperexcitability, but in adults it manifests as migraine, likely due to impaired astrocyte functioning (Benarroch, 2005). That migraineurs display increased infra-slow oscillations directly prior to a migraine headache whilst the individual is pain-free, but in some of the same regions that are subsequently activated during a painful migraine headache, is consistent with the idea that *altered sensitivity in these regions may trigger the migraine itself* or alternatively may reflect altered brainstem “tone” which allows cerebrovascular triggers to evoke an attack.

The restricted nature of regional homogeneity increases during the phase immediately prior to an attack, their overlap with increased infra-slow oscillation power and the increased functional connectivity provide support for a critical role of a PAG–hypothalamic interaction in migraine. The PAG and the posterior hypothalamus have direct neural connections with each other, (Bernard & Bandler, 1998; Floyd et al., 2001) and the increased functional covariation between these regions directly prior to a migraine likely occurs via this direct anatomical connection. A recent case study reported that the hypothalamus showed increased sensitivity to noxious stimuli and greater functional coupling with the dorsomedial pons and SpV during the phase immediately prior to an attack (Schulte & May, 2016). In contrast, we found that functional connectivity changes were restricted to the PAG, hypothalamus, and thalamus during the phase immediately prior to an attack. However, we did not find connectivity changes within lower brainstem regions, despite increased oscillatory changes in the dorsomedial pons and SpV/RVM. A lack of robust signal covariation within the PAG–RVM–SpV circuitry is surprising given its role in modulating incoming noxious information but may stem from the complex interaction between the PAG and the “on” and “off” cells within the RVM. Alternatively, it may be that changes in interactions between the PAG, hypothalamus, and thalamus—in addition to increased regional homogeneity—reflect different roles for these regions in the expression of migraine compared with the lower brainstem.

Finally, there are a number of limitations that need to be acknowledged. First, given the relatively low spatial resolution of resting-state fMRI, it is difficult to accurately localize each cluster to a particular brain nucleus or region. Given that we compared indices across every voxel in the brain and remarkably, those regions previously implicated in migraine were almost exclusively different, we are confident that the locations of the described changes are accurate. However, while we are confident that the cluster locations described in this study include

the regions labeled, most clusters encompassed other adjacent regions and caution must be taken when attributing changes to a single brain region. A second limitation is the modest group sample size and the absence of scans during the headache phase of the migraine cycle. While the results reported here were generated with random-effects, population-based statistics that were corrected for multiple comparisons, future studies with greater sample sizes, particularly in the phase immediately prior to a migraine and during a migraine attack would be extremely valuable.

Our findings provide evidence that brainstem and hypothalamic functions are altered prior to the initiation of the headache, with the temporal and spatial distributions consistent with altered astrocyte function. Whether these central changes are enough in themselves to initiate a migraine attack remains to be determined, although they are consistent with the idea that altered brainstem and hypothalamic activity are potentially involved in the expression of a migraine attack. Understanding how these functional changes precipitate a migraine attack may lead to the development of treatment strategies aimed at the astrocytes, rather than neurons. Indeed, as we learn more about the complexities of glial ion channels and gliotransmission, we may well find means of targeting other forms of pain.

## ACKNOWLEDGMENTS

The authors wish to thank the many volunteers involved in this study. The authors declare that there are no conflicts of interest.

## ORCID

Paul M. Macey  <http://orcid.org/0000-0003-4093-7458>

Luke A. Henderson  <http://orcid.org/0000-0002-1026-0151>

## REFERENCES

- Afridi, S. K., Giffin, N. J., Kaube, H., Friston, K. J., Ward, N. S., Frackowiak, R. S., & Goadsby, P. J. (2005). A positron emission tomographic study in spontaneous migraine. *Archives of Neurology*, *62*(8), 1270–1275.
- Afridi, S. K., Matharu, M. S., Lee, L., Kaube, H., Friston, K. J., Frackowiak, R. S., & Goadsby, P. J. (2005b). A PET study exploring the laterality of brainstem activation in migraine using glyceryl trinitrate. *Brain*, *128*, 932–939.
- Akerman, S., Holland, P. R., & Goadsby, P. J. (2011). Diencephalic and brainstem mechanisms in migraine. *Nature Reviews. Neuroscience*, *12*(10), 570–584.
- Alshelh, Z., Di Pietro, F., Youssef, A. M., Reeves, J. M., Macey, P. M., Vickers, E. R., ... Henderson, L. A. (2016). Chronic neuropathic pain: It's about the rhythm. *Journal of Neuroscience*, *36*(3), 1008–1018.
- Bahra, A., Matharu, M. S., Buchel, C., Frackowiak, R. S., & Goadsby, P. J. (2001). Brainstem activation specific to migraine headache. *Lancet*, *357*(9261), 1016–1017.
- Benarroch, E. E. (2005). Neuron-astrocyte interactions: Partnership for normal function and disease in the central nervous system. *Mayo Clinic Proceedings*, *80*(10), 1326–1338.
- Bernard, J. F., & Bandler, R. (1998). Parallel circuits for emotional coping behaviour: New pieces in the puzzle. *Journal of Comparative Neurology*, *401*(4), 429–436.
- Bernstein, C., & Burstein, R. (2012). Sensitization of the trigeminovascular pathway: Perspective and implications for migraine pathophysiology. *Journal of Clinical Neurology*, *8*(2), 89–99.
- Borsook, D., & Burstein, R. (2012). The enigma of the dorsolateral pons as a migraine generator. *Cephalalgia*, *32*(11), 803–812.
- Burstein, R., Nosedà, R., & Borsook, D. (2015). Migraine: Multiple processes, complex pathophysiology. *Journal of Neuroscience*, *35*(17), 6619–6629.
- Churi, S. B., Abdel-Aleem, O. S., Tumber, K. K., Scuderi-Porter, H., & Taylor, B. K. (2008). Intrathecal rosiglitazone acts at peroxisome proliferator-activated receptor-gamma to rapidly inhibit neuropathic pain in rats. *Journal of Pain*, *9*(7), 639–649.
- Crunelli, V., Blethyn, K. L., Cope, D. W., Hughes, S. W., Parri, H. R., Turner, J. P., ... Williams, S. R. (2002). Novel neuronal and astrocytic mechanisms in thalamocortical loop dynamics. *Philosophical Transactions of the Royal Society B: Biological Sciences*, *357*(1428), 1675–1693.
- Cunningham, M. O., Pervouchine, D. D., Racca, C., Kopell, N. J., Davies, C. H., Jones, R. S., ... Whittington, M. A. (2006). Neuronal metabolism governs cortical network response state. *Proceedings of the National Academy of Sciences of the United States of America*, *103*(14), 5597–5601.
- Denuelle, M., Fabre, N., Payoux, P., Chollet, F., & Geraud, G. (2007). Hypothalamic activation in spontaneous migraine attacks. *Headache: The Journal of Head and Face Pain*, *0*(0), 070503104159006.
- Floyd, N. S., Price, J. L., Ferry, A. T., Keay, K. A., & Bandler, R. (2001). Orbitomedial prefrontal cortical projections to hypothalamus in the rat. *Journal of Comparative Neurology*, *432*(3), 307–328.
- Garrison, C. J., Dougherty, P. M., Kajander, K. C., & Carlton, S. M. (1991). Staining of glial fibrillary acidic protein (GFAP) in lumbar spinal cord increases following a sciatic nerve constriction injury. *Brain Research*, *565*(1), 1–7.
- Giffin, N. J., Ruggiero, L., Lipton, R. B., Silberstein, S. D., Tvedskov, J. F., Olesen, J., ... Macrae, A. (2003). Premonitory symptoms in migraine: An electronic diary study. *Neurology*, *60*(6), 935–940.
- Goadsby, P. J. (2009). The vascular theory of migraine—a great story wrecked by the facts. *Brain*, *132*(Pt 1), 6–7.
- Goadsby, P. J., & Akerman, S. (2012). The trigeminovascular system does not require a peripheral sensory input to be activated—migraine is a central disorder. Focus on 'Effect of cortical spreading depression on basal and evoked traffic in the trigeminovascular sensory system'. *Cephalalgia*, *32*(1), 3–5.
- Goadsby, P. J., Charbit, A. R., Andreou, A. P., Akerman, S., & Holland, P. R. (2009). Neurobiology of migraine. *Neuroscience*, *161*(2), 327–341.
- Halassa, M. M., Fellin, T., & Haydon, P. G. (2007). The tripartite synapse: Roles for gliotransmission in health and disease. *Trends in Molecular Medicine*, *13*(2), 54–63.
- Holstege, G., & Kuypers, H. G. (1982). The anatomy of brain stem pathways to the spinal cord in cat. A labeled amino acid tracing study. *Progress in Brain Research*, *57*, 145–175.
- Hubbard, J. A., & Binder, D. K. (2016). *Astrocytes and epilepsy*. Academic Press.
- Hughes, S. W., Lorincz, M. L., Parri, H. R., & Crunelli, V. (2011). Infralow (<0.1 Hz) oscillations in thalamic relay nuclei basic mechanisms and significance to health and disease states. *Progress in Brain Research*, *193*, 145–162.
- James, M. F., Smith, J. M., Boniface, S. J., Huang, C. L., & Leslie, R. A. (2001). Cortical spreading depression and migraine: New insights from imaging? *Trends in Neuroscience*, *24*(5), 266–271.
- Ji, X. T., Qian, N. S., Zhang, T., Li, J. M., Li, X. K., Wang, P., ... Niu, L. (2013). Spinal astrocytic activation contributes to mechanical

- allodynia in a rat chemotherapy-induced neuropathic pain model. *PLoS One*, 8(4), e60733.
- Knight, Y. E., & Goadsby, P. J. (2001). The periaqueductal grey matter modulates trigeminovascular input: A role in migraine? *Neuroscience*, 106(4), 793–800.
- Lambert, G. A., Truong, L., & Zagami, A. S. (2011). Effect of cortical spreading depression on basal and evoked traffic in the trigeminovascular sensory system. *Cephalalgia*, 31(14), 1439–1451.
- Linde, M., Mulleners, W. M., Chronicle, E. P., & McCrory, D. C. (2013). Valproate (valproic acid or sodium valproate or a combination of the two) for the prophylaxis of episodic migraine in adults. *Cochrane Database of Systematic Reviews*, CD010611.
- Lorincz, M. L., Geall, F., Bao, Y., Crunelli, V., & Hughes, S. W. (2009). ATP-dependent infra-slow (<0.1 Hz) oscillations in thalamic networks. *PLoS One*, 4(2), e4447.
- Macey, P. M., Macey, K. E., Kumar, R., & Harper, R. M. (2004). A method for removal of global effects from fMRI time series. *NeuroImage*, 22(1), 360–366.
- Mai, J. K., Paxinos, G., & Voss, T. (2007). *Atlas of the human brain*. Academic Press.
- Mantini, D., Perrucci, M. G., Del Gratta, C., Romani, G. L., & Corbetta, M. (2007). Electrophysiological signatures of resting state networks in the human brain. *Proceedings of the National Academy of Sciences of the United States of America*, 104(32), 13170–13175.
- Marciszewski, K. K., Meylakh, N., Di Pietro, F., Macefield, V. G., Macey, P. M., & Henderson, L. A. (2017). Altered brainstem anatomy in migraine. *Cephalalgia*, 33(10), 1769–1784.
- Morgan, M. M., Whittier, K. L., Hegarty, D. M., & Aicher, S. A. (2008). Periaqueductal gray neurons project to spinally projecting GABAergic neurons in the rostral ventromedial medulla. *Pain*, 140(2), 376–386.
- Morgenweck, J., Griggs, R. B., Donahue, R. R., Zadina, J. E., & Taylor, B. K. (2013). PPARgamma activation blocks development and reduces established neuropathic pain in rats. *Neuropharmacology*, 70, 236–246.
- Nedergaard, M., Cooper, A. J., & Goldman, S. A. (1995). Gap junctions are required for the propagation of spreading depression. *Journal of Neurobiology*, 28(4), 433–444.
- Okada-Ogawa, A., Suzuki, I., Sessle, B. J., Chiang, C. Y., Salter, M. W., Dostrovsky, J. O., ... Iwata, K. (2009). Astroglia in medullary dorsal horn (trigeminal spinal subnucleus caudalis) are involved in trigeminal neuropathic pain mechanisms. *Journal of Neuroscience*, 29(36), 11161–11171.
- Parri, H. R., & Crunelli, V. (2001). Pacemaker calcium oscillations in thalamic astrocytes in situ. *NeuroReport*, 12(18), 3897–3900.
- Parri, H. R., Gould, T. M., & Crunelli, V. (2001). Spontaneous astrocytic Ca<sup>2+</sup> oscillations in situ drive NMDAR-mediated neuronal excitation. *Nature Neuroscience*, 4(8), 803–812.
- Paxinos, G., & Huang, X. (1995). *Atlas of the human brainstem*. San Diego, CA: Academic Press.
- Schulte, L. H., & May, A. (2016). The migraine generator revisited: Continuous scanning of the migraine cycle over 30 days and three spontaneous attacks. *Brain*, 139(7), 1987–1993.
- Shi, Y., Gelman, B. B., Lisinicchia, J. G., & Tang, S. J. (2012). Chronic-pain-associated astrocytic reaction in the spinal cord dorsal horn of human immunodeficiency virus-infected patients. *Journal of Neuroscience*, 32(32), 10833–10840.
- Stankewitz, A., Aderjan, D., Eippert, F., & May, A. (2011). Trigeminal nociceptive transmission in migraineurs predicts migraine attacks. *Journal of Neuroscience*, 31(6), 1937–1943.
- Strassman, A., Mason, P., Moskowitz, M., & Maciewicz, R. (1986). Response of brainstem trigeminal neurons to electrical stimulation of the dura. *Brain Research*, 379(2), 242–250.
- Strassman, A. M., Mineta, Y., & Vos, B. P. (1994). Distribution of FOS-like immunoreactivity in the medullary and upper cervical dorsal horn produced by stimulation of dural blood vessels in the rat. *Journal of Neuroscience*, 14, 3725–3735.
- Tian, G. F., Azmi, H., Takano, T., Xu, Q., Peng, W., Lin, J., ... Nedergaard, M. (2005). An astrocytic basis of epilepsy. *Nature Medicine*, 11(9), 973–981.
- Vanhatalo, S., Palva, J. M., Holmes, M. D., Miller, J. W., Voipio, J., & Kaila, K. (2004). Infralow oscillations modulate excitability and interictal epileptic activity in the human cortex during sleep. *Proceedings of the National Academy of Sciences of the United States of America*, 101(14), 5053–5057.
- Veloso, F., Kumar, K., & Toth, C. (1998). Headache secondary to deep brain implantation. *Headache: The Journal of Head and Face Pain*, 38(7), 507–515.
- Wang, C. C., Chen, P. S., Hsu, C. W., Wu, S. J., Lin, C. T., & Gean, P. W. (2012). Valproic acid mediates the synaptic excitatory/inhibitory balance through astrocytes—a preliminary study. *Progress in Neuro-Psychopharmacology & Biological Psychiatry*, 37(1), 111–120.
- Weiller, C., May, A., Limmroth, V., Juptner, M., Kaube, H., Schayck, R. V., ... Diener, H. C. (1995). Brain stem activation in spontaneous human migraine attacks. *Nature Medicine*, 1(7), 658–660.

**How to cite this article:** Meylakh N, Marciszewski KK, Di Pietro F, Macefield VG, Macey PM, Henderson LA. Deep in the brain: Changes in subcortical function immediately preceding a migraine attack. *Hum Brain Mapp*. 2018;39:2651–2663. <https://doi.org/10.1002/hbm.24030>